A SED-based approach to predict the fatigue strength of notched and plain shot-peened parts

M. Benedetti[1], M. Bandini[2], S. Raghavendra[1], V. Fontanari[1], and F. Berto[3]

1 Department of Industrial Engineering, University of Trento, Italy
2 PeenService, Bologna, Italy
3 Dep. of Mechanical and Industrial Engineering, Norwegian University of Science and Technology, Norway

Abstract
A Strain Energy Density (SED) based fatigue criterion is developed to incorporate residual stresses (RS). Mechanical and residual stresses are treated separately. The formers are encapsulated in the form of SED associated to stress range and maximum SED. The work done when tensile mechanical strains fluctuate in the presence of compressive RS is added to the equivalent SED of the fatigue criterion. This is calibrated and validated using the results of an extensive experimental campaign aimed at exploring the effect of shot-peened induced RS on plain and notch fatigue strength of Al-7075-T651.

Keywords Strain energy density; Notch fatigue assessment; Residual stresses; Shot peening.

Introduction

Shot peening is a widely used surface treatment known to greatly improve the fatigue strength of machine elements, especially in the presence of stress raisers [1]. Its beneficial effect is mainly related to the introduction of compressive residual stresses (RS) into the surface layer. A reliable fatigue calculation method of shot-peened parts necessitates the incorporation of residual stresses into a suitable fatigue criterion. In stress-based approaches, RS are treated as mean stresses superimposed to the external stress field. Sometimes, the notch effect is accounted for according to the Theory of Critical Distances. In fracture mechanics approaches, RS are encapsulated into the definition of a closure stress intensity factor that reduces the effective stress intensity range available for the fatigue crack propagation. In recent years, the concept of strain energy density (SED) emerged as a very promising theoretical framework for accurate fatigue calculations [2]. However, to the authors' best knowledge, none attempted so far to incorporate shot-peening RS into the definition of SED.

Definition of the SED fatigue criterion

An exhaustive explanation of the theoretical framework of the SED approach to notch fatigue assessment can be found in [2]. In essence, the underpinning concept is that the fatigue damage is controlled by the SED averaged over a control volume Ω of material characteristic size. For plane or axisymmetric problems, the control volume simplifies into a circular domain, as schematically illustrated in Fig. 1a. In the classical formulation of the method, the fatigue damage is linked to the variation between maximum and minimum SED occurring during the load cycle. To take into account the mean stress effect, the authors proposed in [3] to incorporate the range $\Delta\overline{W}$ and the maximum value $\overline{W}_{\max}$ of the average SED into a Walker-like equation to express an equivalent fatigue damage parameter:

$$\Delta\overline{W}_{eq} = \Delta\overline{W}^{\alpha}\overline{W}_{\max}^{1-\alpha} = \Delta\overline{W}_{1} \tag{1}$$

The SED components are graphically illustrated in Fig. 1b by the dashed and grey area, respectively, in the simple case of uniform uniaxial stress. The overbar sign indicates that

the two SED components are averaged over the same domain Ω in the case of a non-uniform stress distribution occurring in the vicinity of notches. The mean stress sensitivity factor 1-α, the control radius R_1 and the fatigue strength characteristic $\Delta\overline{W}_1$ are material-dependent constants, which are assumed to depend only on the number of cycles to failure N_f. They must be calibrated using at least three experimental fatigue data. In this paper, we propose to conceive RS as a stress field independent of the external one. As schematically shown in Fig. 1c in the simple case of uniaxial stress, when tensile mechanical strains fluctuate in the presence of compressive RS, a negative specific work is done and expressed as:

$$W^{RS} = \sigma^{RS}\Delta\varepsilon^{+}$$
$$\Delta\varepsilon^{+} = \begin{cases} \varepsilon_{\max} - \varepsilon_{\min} & \varepsilon_{\min} > 0 \\ \varepsilon_{\max} & \varepsilon_{\min} \le 0 \end{cases} \quad (2)$$

The RS specific work $\overline{W}^{RS}$ expressed by Eq. (2) and averaged over the domain Ω reduces the SED associated to the external stresses, thus accounting for the beneficial effect of compressive RS. Therefore, we propose to incorporate RS into the fatigue criterion simply by including $\overline{W}^{RS}$ in $\Delta\overline{W}_{eq}$:

$$\Delta\overline{W}_{eq}^{RS} = \Delta\overline{W}^{\alpha}\overline{W}_{\max}^{1-\alpha} + \overline{W}^{RS} = \Delta\overline{W}_1 \quad (3)$$

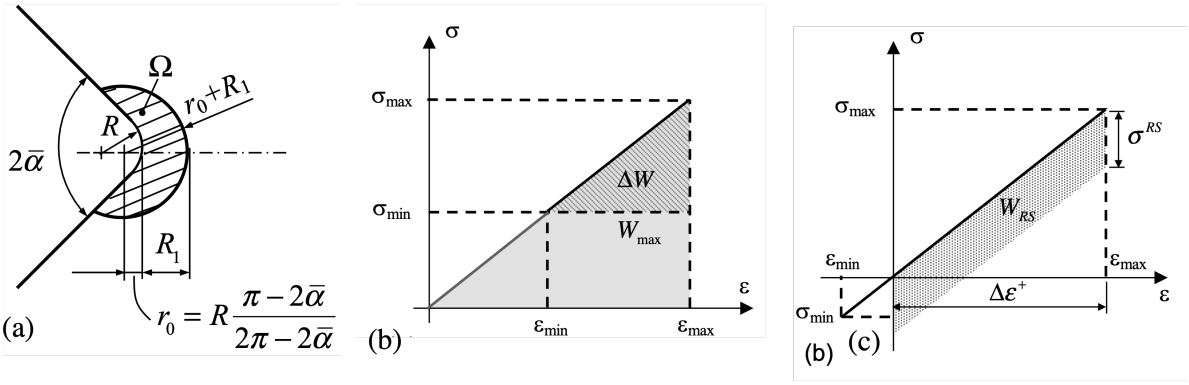

Fig. 1. (a) Strain energy density averaging domain Ω (dashed area) ahead of the notch root in the case of plane or axisymmetric problems. (b) SED components associated to the external mechanical loading, viz. SED associated to the stress range ΔW (dashed area) and maximum SED $W_{\max}$ (grey area). (c) Specific work W^{RS} done by fluctuating positive mechanical strains in the presence of residual stresses.

Material and experimental procedures

An extensive experimental testing campaign was carried out in the past with the aim of investigating the effect of shot peening on plain and fatigue strength of Al alloys. Details regarding the material and experimental procedures used to generate the fatigue data analyzed in this article can be found in [4,5,6,7]. In brief, the experimentation was performed on the aeronautical grade Al-7075-T651 aluminum alloy supplied in the form of 4 mm thick rolled plate. Characteristic dimensions are listed in Table 1. Plain (smooth) and notched prismatic specimens with three increasing levels of notch severity were machined. A schematic view of specimens' geometry is provided in Fig. 2. Part of the specimens were subject to a gentle shot peening treatment termed B120 (ceramic beads of 120 μm diameter, Almen intensity 10N). The specimens were fatigued under bending loading (about *y*-axis, see Fig. 3) at two load ratios R, namely -1 and 0.05.

RS measurements were carried out in [8] in the vicinity of the notch tip in notched samples and of the lateral edge in smooth samples (where fatigue crack initiation occurs) through two complementary experimental techniques, namely micro-XRD and micro-hole drilling/slot cutting. RS measurements were undertaken in non-tested samples as well as in samples fatigued at two load levels for a number of cycles equal to 50% of the expected fatigue life, viz. 2×10^5 and 2×10^6 cycles, respectively. Such measurements were used to reconstruct the RS field in the vicinity of the notch tip according to the eigenstrain method illustrated in [9]. In brief, this consists in the superposition of the misfit strains produced by two fictitious temperature distributions, whose intensity and spatial distribution were deduced by fitting the experimental data after being corrected for the radiation penetration depth.

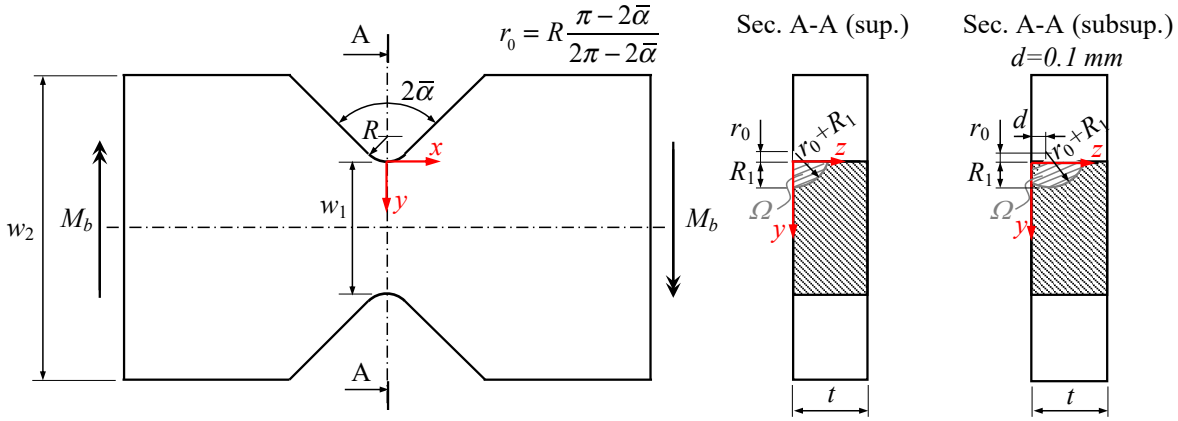

Fig.2. Geometry of the prismatic samples used for the fatigue tests. Characteristic dimensions are listed in Table 1. The SED-averaging control domain Ω is centered either on the frontal tensioned side of the specimen ("sup.") or at distance *d* from this plane ("subsup.").

Table 1. Fatigue sample designation and geometry. See Fig. 2 for the meaning of the geometrical parameters.

Designation	w_1 (mm)	w_2 (mm)	t (mm)	$2\bar{\alpha}$ (°)	R (mm)
Plain (R30)	6	12	4	90	30
Smooth (R2)					2
Sharp (R0.5)					0.5
Ultra-sharp (R0.15)					0.15

Experimental Results

The results of the fatigue tests are shown in Fig. 3a and b, for pulsating (R=0.05) and fully-reversed (R=-1) bending loading, respectively. Solid and open symbols refer to as-received and peened conditions, respectively. Run-out tests are marked by arrows. Solid lines represent best-fit curves, corresponding to 50% failure probability. The scatter of the fatigue data was estimated by computing the regression variance assumed to be uniform for the whole fatigue curve and used to draw the fatigue curves (dashed lines) corresponding to 10% and 90% failure probability. It can be noted that the shot peening treatment is beneficial to the fatigue strength, especially in the presence of stress raisers. Moreover, the fatigue improvement increases with notch severity and is higher under fully-reversed rather than pulsating bending fatigue. Importantly, in the very high-cycle fatigue (VHCF) regime explored in pulsating bending fatigue tests, the improvement imparted by shot peening at shorter fatigue lives is retained in the sharp and ultra-sharp notched conditions, whereas it is almost lost or reduced to 20% in plain and blunt-notched specimens, respectively.

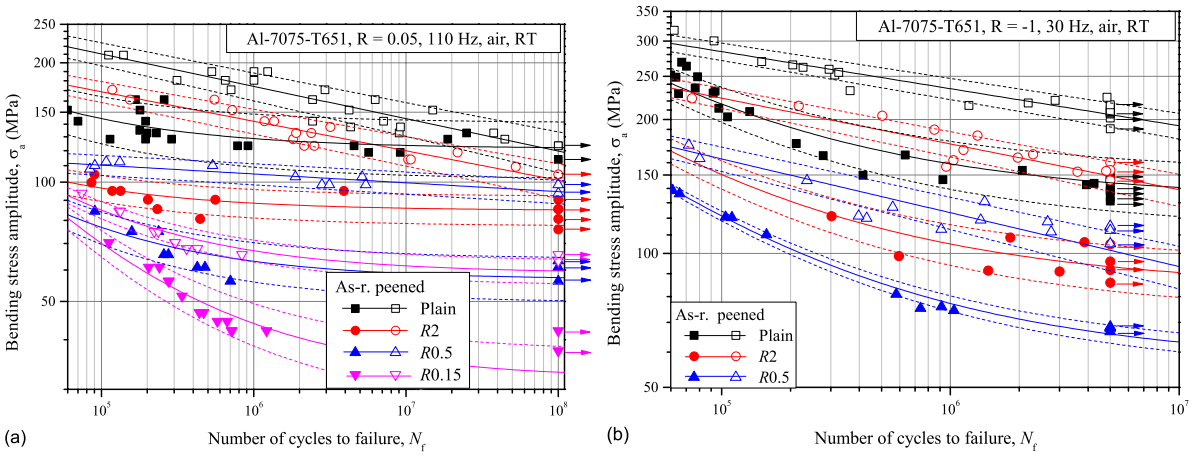

Fig. 3. Bending fatigue curves of the plain and notched specimens: (a) pulsating, (b) fully-reversed fatigue tests. Run-out tests are marked by arrows. Data of as-received samples are indicated as ‘‘As-r.” in figures’ legend. Solid lines represent 50% failure probability, while dashed lines refer to 10% and 90% failure probability.

Discussion and Conclusions

The obtained fatigue results are here reinterpreted on the base of the proposed SED fatigue calculation approach. For this purpose, a 2D domain consisting in a circular sector centered in the origin of the notch curvilinear reference frame, a circular domain Ω lying on the symmetry plane *yz* is considered. The location of this domain with respect to the specimen thickness (*z*-axis) is set according to the expected position of the fatigue crack initiation site. Fractographic inspections [6,7] revealed that the majority of cracks nucleated very close to the tensioned frontal surface of the samples. In this scenario, denoted as "sup." in Fig. 2, the center of Ω is coplanar with the tensioned frontal surface. Since plain and blunt-notched samples tested in the VHCF regime exhibited a tendency towards sub-superficial crack initiation (about 0.1 mm below the outer surface), the center of Ω is moved 0.1 mm beneath the tensioned surface to account for this scenario, indicated as "subsup." in Fig. 2. The range (maximum value) of the SED associated to mechanical loading is computed via FEM for each element lying in the control volume in terms of range (maximum value) of stress and elastic strain components. These element SED components are finally used to compute the corresponding SED components averaged over the control volume $\Delta\overline{W}$ and $\overline{W}_{\max}$. The RS specific work $\overline{W}^{RS}$ is calculated by means of FE models, wherein RS are introduced by means of two independent temperature fields. After introducing the bending load in the same manner described above, the positive range of elastic strains and the corresponding RS components are evaluated, whereby $\overline{W}^{RS}$ is averaged on the domain Ω. Fatigue calculations of shot peened variants will be done incorporating either initial (IRS) or stabilized (SRS, partially relaxed) residual stresses. The tri-parametric fatigue criterion is calibrated by least-square fitting the unpeened fatigue data to get a robust determination of material dependent parameters R1, α and $\Delta\overline{W}_1$. Figure 4a and b compare experimental data and SED predictions in the whole explored fatigue regime for load ratios R=0.05 and R=-1, respectively, considering either SRS (solid lines) and IRS (dash-dotted lines). Looking at Fig. 4b, the very good agreement between calculations (made under the assumption of superficial crack initiation) and experiments is evident in the whole explored fatigue range ($5\times10^4<N_f<5\times10^6$) for all the specimen geometries. SRS calculations are in better agreement with experimental data with respect to IRS, especially in the medium-to-high cycle fatigue (M-HCF) regime, where more intense RS relaxation takes place. Looking at Fig. 4a (R=0.05), the discrepancy of IRS from the experimental data of the notched variants is much more pronounced, suggesting that cyclic RS relaxation plays a crucial role in dictating the pulsating fatigue strength in the presence of stress raisers. If we look at SRS predictions

reported in Fig. 4a, where the fatigue tests were prolonged until 1×10^8 cycles, the scenario is different from that shown in Fig. 4b.

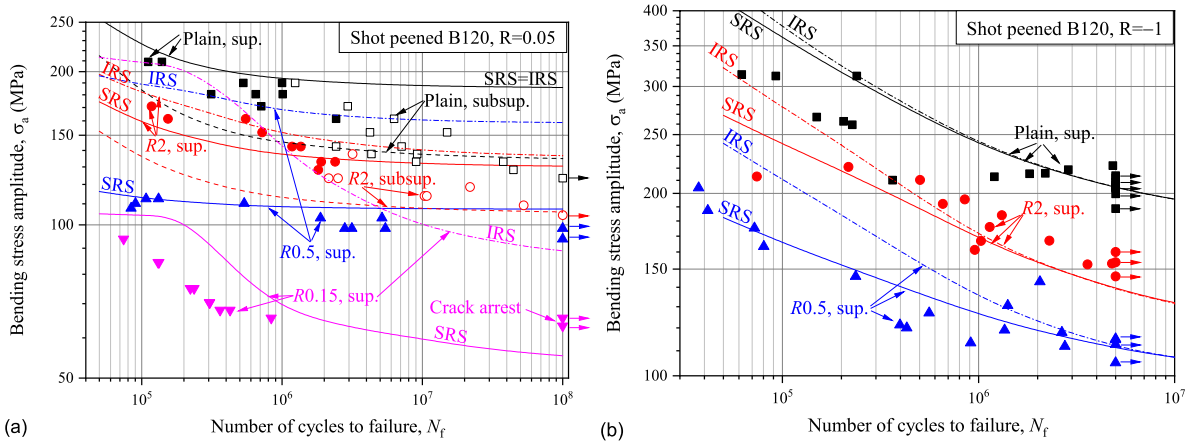

Fig. 4. Assessment of the fatigue curves of shot-peened samples under (a) pulsating and (b) fully-reversed bending fatigue. Solid and dash-dotted lines indicate fatigue predictions incorporating stabilized and initial RS. "Sup." and "subsup." refer to fatigue calculations done on or 0.1 mm below the tensioned frontal surface, respectively. "Crack arrest" denotes experimental evidences of non-propagating crack at the tip of the ultra-sharp-notched specimens (Fig. 5a). The points indicate to the experimental data.

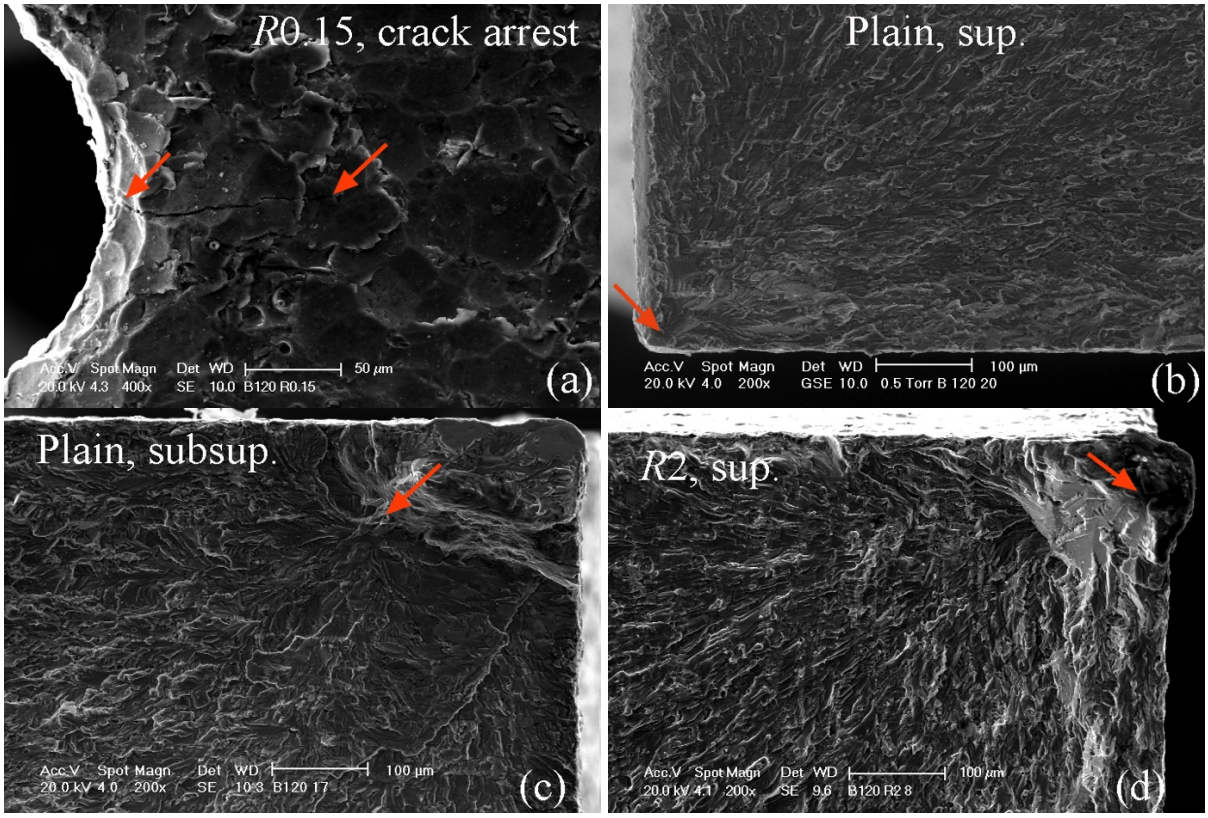

Fig. 5. SEM micrographs of peened samples. (a) non-propagating crack nucleated at the tip of the ultra-sharp-notched specimen. (b)-(d) Fracture surface in the vicinity of the crack initiation site marked by a red arrow. (b) Superficial and sub-superficial (c) crack initiation in plain samples, (d) *R*2 blunt-notched. All samples were tested at R=0.05.

The sharp-notched (R0.5) variant is accurately assessed in the entire fatigue range, the ultra-sharp notched (R0.15) one is very well assessed in the central part of the SN diagram

($1\times10^6<N_f<1\times10^7$), while the medium and the very-high-cycle fatigue regimes are overestimated and underestimated, respectively. This underestimation can be ascribed to the presence of non-propagating cracks nucleated at the notch root in run-out specimens, as shown in the SEM micrograph reported in Fig. 5a. In other words, the devised fatigue criterion can accurately estimate the surface crack initiation in ultra-sharp notched specimens, but the intense RS stress field along with the pronounced external stress gradient ahead of the notch tip is able to arrest the crack after nucleation. In brief, notches of high severity favor crack initiation in the vicinity of the notch tip lying on the frontal tensioned surface of the specimen. Conversely, the plain and blunt-notched (R2) variants tested at R=0.05 presents a much more complicated situation. In the medium cycle fatigue regime ($Nf<1\times10^6$), fatigue cracks tend to nucleate in the vicinity of the tensioned surface, as shown in fractographs reported in Fig. 5b and 5d, respectively. Therefore, it is not surprising that assessments made according to the "sup." calculation method are in good agreement with the experimental data in this fatigue regime. In the HCF and mostly in the VHCF regime, this calculation method yields less and less accurate estimations of the fatigue strength. The experimental data progressively approaches the assessments done with the "subsup." SED-approach, thus suggesting that in this fatigue regime crack initiation is more prone to happen in the sub-superficial layers below that affected by compressive RS, as confirmed by fractographs depicted in Fig. 5c and d, for plane and blunt-notched specimens. This evidence highlights the importance of correctly identifying the crack initiation site for an accurate fatigue prognosis, given the tendency of shot peened components towards sub-superficial crack nucleation.

References

[1] S. Bagherifard, *Enhancing the Structural Performance of Lightweight Metals by Shot Peening*, Advanced Engineering Materials, Vol. 21 (2019), 1801140.

[2] F. Berto and P. Lazzarin, *Recent developments in brittle and quasi-brittle failure assessment of engineering materials by means of local approaches*, Mater. Sci. Eng R, Vol. 75 (2014), pp. 1–48.

[3] M. Benedetti, F. Berto, L. Le Bone and C. Santus, *A novel Strain-Energy-Density based fatigue criterion accounting for mean stress and plasticity effects on the medium-to-high-cycle uniaxial fatigue strength of plain and notched components*, Int J Fatigue, Vol. 133 (2020), 105397.

[4] M. Benedetti, V. Fontanari, P. Scardi, C.L.A. Ricardo and M. Bandini, *Reverse bending fatigue of shot peened 7075–T651 aluminium alloy: the role of residual stress relaxation*, Int J Fatigue, Vol. 31 (2009), pp. 1225–1236.

[5] M. Benedetti, V. Fontanari, C. Santus and M. Bandini, *Notch fatigue behaviour of shot peened high-strength aluminium alloys: experiments and predictions using a critical distance method*, Int J Fatigue, Vol. 32 (2010), pp. 1600–1611.

[6] M. Benedetti, V. Fontanari, M. Allahkarami, J.C. Hanan and M. Bandini, *On the combination of the critical distance theory with a multiaxial fatigue criterion for predicting the fatigue strength of notched and plain shot-peened parts*, Int J Fatigue, Vol. 93(2016), pp. 133–47.

[7] M. Benedetti, V. Fontanari, M. Bandini and E. Savio, *High- and very high-cycle plain fatigue resistance of shot peened high-strength aluminum alloys: the role of surface morphology*, Int J Fatigue, Vol. 70 (2015), pp. 451–462.

[8] B. Winiarski, M. Benedetti, V. Fontanari, M. Allahkarami, J.C. Hanan and P. J. Withers, *High spatial resolution evaluation of residual stresses in shot peened specimens containing sharp and blunt notches by micro-hole drilling, micro- slot cutting and micro-X-ray diffraction methods*, Exp Mech, Vol. 56 (2016), pp. 1449-1463.

[9] M. Benedetti, V. Fontanari, B. Winiarski, M. Allahkarami and J.C. Hanan, *Residual stresses reconstruction in shot peened specimens containing sharp and blunt notches by experimental measurements and finite element analysis*, Int J Fatigue, Vol. 87 (2016), pp. 102–111.